Proceedings of the
44th IEEE Conference on Decision and Control, and
the European Control Conference 2005
Seville, Spain, December 12-15, 2005

Robust Acceleration Control of Electrodynamic Shaker Using μ–Synthesis

Yasuhiro Uchiyama, Masakazu Mukai, and Masayuki Fujita

Abstract— **This paper presents an acceleration control of an electrodynamic shaker that cannot employ the iteration control method freely. There are considerable points in the design phase of the acceleration controller. The transfer functions using the acceleration controlled variable have zero at the origin and two crossover frequencies. It is not easy to design the acceleration controller by using the conventional design method directly. The controller is designed by using μ–synthesis based on these points. Further, a two degrees of freedom controller is designed to improve the transient response. Finally, the experiment using an actual electrodynamic shaker is carried out. A comparison between the proposed controller and the controller derived from the iteration control method is shown.**

I. INTRODUCTION

Recently, multi-axis shaking tables which more accurately can replicate an actual situation are being widely used. For instance, the shaker is used in automotive industry, civil and architectural engineering, etc. An electrohydraulic shaker was generally used for a large-scale multi-axis shaking table. An electrodynamic shaker has some good features such as good linearity and a wide-frequency response. A more accurate vibration test can be realized when the multi-axis shaking table is comprised by electrodynamic shakers. Further, by having the feature of the wide-frequency response, acceleration is generally used to control the electrodynamic shaker. Then, the importance of the acceleration control is emphasized.

The controller of the multi-axis shaker is required to provide not only stable control but also a good replication of the given reference waveform as a response waveform to the movement associated with the shaking table. Conventional controllers employ the open-loop method by using iterative compensation through repetitive excitations. Since the damage for a specimen is accumulated at each iteration before the execution of the desired excitation, the application of the iterative compensation is undesirable. Furthermore, in the case that the test piece is easy to break, the iteration control cannot be applied. Thus, a new method without iteration control recently attracts attention. On the other hand, an experimental method, like the simulation of soil-structure interaction effects [1], in which an actual vibration test and a computer simulation are combined, recently tends to increase. In this method, it is necessary to control a shaker in real time without delaying the computer simulation. However, the conventional controller of an electrodynamic shaker is based on a feedforward control using an FFT and can update only the drive signal per frame time of the FFT. Hence, it is difficult to employ the conventional controller in this method.

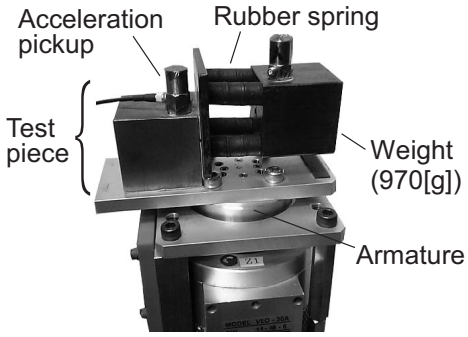

Fig. 1. Electrodynamic shaker with a specimen (VEO-30).

In the examples of the control applications for the electrodynamic shaker, an adaptive inverse control has been successfully applied for the shock testing [2], and the implementation of the current and acceleration controllers can achieve good random vibration control [3]. However, since the test applications are different from this case, the approaches are not appropriate in this case. In contrast, there are some instances with the electrohydraulic shaker. For example, the MCS (Minimal Control Synthesis) method, one of the model reference adaptive control methods, has successfully been applied [4], the application of H_∞ control has extended the frequency response of shaking table [5], and the compensator by an adaptive filter has improved the control results, the real-time compensator of a reaction force has cancelled out its influence [6]. In our previous studies [7], [8], a good performance is achieved for the control of the electrodynamic shaking system. Since the design is for general case and there are abundant examples of the control application, the displacement is used as the controlled variable in [7], [8]. However, the vibration test cannot be executed at higher frequency band which is the advantage of the electrodynamic shaker and the prospective application using the displacement control is restricted.

In this paper, an acceleration control of the electrodynamic shaker (Fig. 1) is presented. The final purpose of this study is to construct the controller of multi-axis shaking system. However, in this paper, due to mainly design and evaluate

Y. Uchiyama is with IMV CORPORATION, Osaka 555-0011, JAPAN uchiyama@imv.co.jp

M. Mukai is with the Department of Electrical and Electronic Systems Engineering, Graduate School of Information Science and Electrical Engineering, Kyushu University, Fukuoka 812-8581, JAPAN

M. Fujita is with the Department of Mechanical and Control Engineering, Tokyo Institute of Technology, Tokyo 152-8552, JAPAN

0-7803-9568-9/05/$20.00 ©2005 IEEE

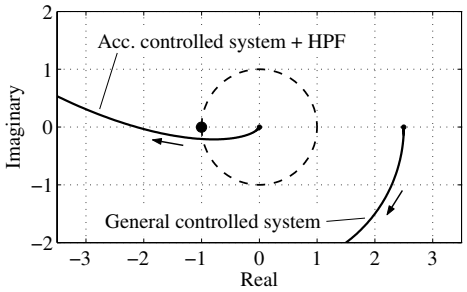

Fig. 2. Nyquist diagram of general control and acceleration control in lower frequency.

the acceleration controller, a single-axis compact shaker is used. There are considerable points in the design phase of the acceleration controller. The transfer functions using the acceleration controlled variable have zero at the origin and two crossover frequencies. The controller is designed by using μ–synthesis based on these points. The experiment using an actual electrodynamic shaker is carried out to illustrate the effect of the proposed controller. Then a comparison between the proposed controller and the controller derived from the iteration control method is shown based on these experimental results.

II. THE CONTROL PROBLEM

In acceleration control, a few attention should be paid to the following points:

1) The controlled system has zero at $s = 0$.
2) There exist two crossover frequencies.
3) The response in lower frequency is influenced by noise.

In the item 1), to satisfy the assumptions of the standard H_∞ control problem [9], it is meant that a weighting function and a constitution of the generalized plant is constrained.

Nyquist diagram of two systems in lower frequency is shown in Fig. 2. In the general controlled system, the locus of the open-loop characteristic starts from the point greater than 1 on the real axis, and the system has one crossover frequency. However, in the case of the acceleration controlled system to which is added the high pass filter characteristic like the AC coupling, the locus is drawn as shown in Fig. 2, and it is found that the system has two crossover frequencies. Therefore, it is needed that the stability margins at lower and higher crossover frequency are considered as the item 2).

Generally, the noise in higher frequency band is cared when a controller is designed. Since the gain of the acceleration controlled system is small in lower frequency, the problem of the item 3) is occurred easily. Thus, the noise in lower frequency band should be cared, too.

III. ELECTRODYNAMIC SHAKER MODEL

It is difficult to express the precise characteristic of an actual plant by using a mathematical model, and some uncertainties are generally present. In this section, a nominal model of an electrodynamic shaker and an uncertainty weighting function are introduced.

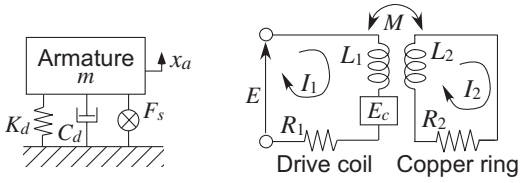

Fig. 3. Schematic diagram of the armature and the equivalent circuit.

A. Nominal model

The plant to be controlled is an electrodynamic shaker depicted in Fig. 1. The electrodynamic shaker is based on the principle that an electrodynamic force is generated in proportion to an electric current applied to the coil existing in the magnetic field. The simplified model of the electrodynamic shaker can be shown as a vibration system with a single degree of freedom. Assuming that the magnetic flux density is constant, a drive coil can be shown as a linear equivalent circuit. The schematic model of the shaker and the equivalent circuit are depicted in Fig. 3. The force F_s and the reverse electromotive force E_c can be represented as

$$F_s = BlI_1 \tag{1}$$

$$E_c = Bl\dot{x}_a, \tag{2}$$

where x_a denotes the displacement of the armature, I_1 denotes the current of the drive coil, l denotes the length of the drive coil, and B denotes the magnetic flux density. From Fig. 3, the following (3) and (4) can be obtained

$$E = R_1 I_1 + L_1 \dot{I}_1 + E_c + M\dot{I}_2 \tag{3}$$

$$0 = R_2 I_2 + L_2 \dot{I}_2 + M\dot{I}_1, \tag{4}$$

where M denotes a relative inductance, I_2 denotes the current of the copper ring, $L_{1,2}$ denote an inductance, $R_{1,2}$ denote a resistance, and E denotes the input voltage to the drive coil. The dynamic equation of the armature can be obtained as

$$F_s = m\ddot{x}_s + C_d\dot{x}_a + K_d x_a, \tag{5}$$

where K_d denotes the stiffness coefficient of the suspension, and C_d denotes the damping coefficient of the suspension. Considering the voltage u_a as input and the acceleration $\ddot{x}_a$ as output, the characteristic of the electrodynamic shaker can be represented as the following state-space form

$$\begin{aligned}
&\dot{x} = A_a x + B_a u_a, \quad y_a = C_a x_a,\\
&x = \left[x_a \;\; \dot{x}_a \;\; I_1 \;\; I_2\right],\\
&A_a = \begin{bmatrix} 0 & 1 & 0 & 0 \\ -\frac{K_d}{m} & -\frac{C_d}{m} & \frac{Bl}{m} & 0 \\ 0 & -\frac{BlL_2}{L_1L_2-M^2} & -\frac{R_1L_2}{L_1L_2-M^2} & \frac{MR_2}{L_1L_2-M^2} \\ 0 & \frac{BlM}{L_1L_2-M^2} & \frac{MR_1}{L_1L_2-M^2} & -\frac{L_1R_2}{L_1L_2-M^2} \end{bmatrix},\\
&B_a = \begin{bmatrix} 0 & 0 & \frac{G_aL_2}{L_1L_2-M^2} & -\frac{G_aM}{L_1L_2-M^2} \end{bmatrix}^T,\\
&C_a = \begin{bmatrix} -\frac{K_d}{m} & -\frac{C_d}{m} & \frac{Bl}{m} & 0 \end{bmatrix},
\end{aligned} \tag{6}$$

where G_a denotes the amplifier gain.

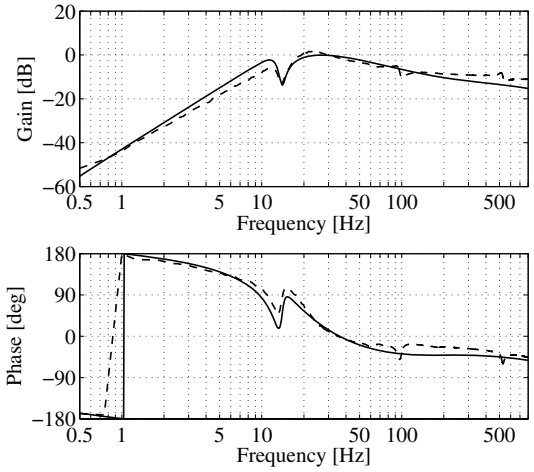

Fig. 4. Bode diagram of the shaker system (solid line: simulated value, dashed line: measured result).

TABLE I

PERTURBED PARAMETERS.

Symbol	Perturbation region
R_1	-4 – 10%
L_1	-30 – 30%
B	-10 – 10%
K_d	-5 – 5%
C_d	-10 – 10%
m	-10 – 10%
R_2	-10 – 10%
L_2	-30 – 30%

In Fig. 1, a specimen constructed by a 970 g weight and rubber springs are located on an armature. The first-order resonant frequency of the specimen is approximately 13 Hz. Due to the influence of the resonance, a peak notch appeared in the transfer characteristic of the shaker in the neighborhood of the resonant frequency. In this paper, the influence of the specimen is approximated by the following (7).

$$G_e = \frac{s^2 + 2\zeta_2\omega_2 s + \omega_2^2}{s^2 + 2\zeta_1\omega_1 s + \omega_1^2}, \tag{7}$$

where $\omega_1 = 2\pi \cdot 12.8$, $\zeta_1 = 0.15$, $\omega_2 = 2\pi \cdot 14$, $\zeta_2 = 0.04$. Although the peak notch characteristic at 100 Hz and 550 Hz can be represented by using the form (7), these characteristics are considered as an uncertainty.

Add a high pass filter that has the cutoff frequency 0.15 Hz as the AC coupling. The bode diagram of the model is shown in Fig. 4. In Fig. 4, the solid line denotes the simulated value and the dashed line denotes the measured result. In addition, the characteristic of an antialiasing filter and the AC coupling of the amplifier are added to the transfer function (6) and (7). Then the resulting model is defined as the nominal model G_s.

B. Modeling uncertainty

In this study, the parameter perturbations of the shaker and the influence of the peak notch characteristic which is neglected are considered as an unstructured additive perturbation. To estimate the quantities of additive model

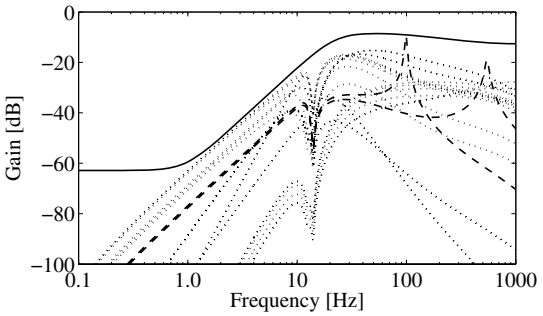

Fig. 5. Uncertainty weighting W_d and additive perturbations (solid line: W_d, dotted line: parameter perturbation, dashed line: influence of the peak notch characteristic).

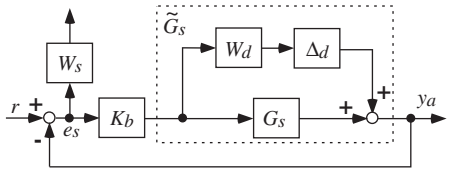

Fig. 6. Feedback structure.

perturbations, the differences between the nominal transfer function and the perturbed transfer functions are calculated when only one parameter is changed and the others are fixed. The parameter perturbations are shown in Table I. According to the perturbation, 16 perturbed models can be obtained. In addition, the influence of the peak notch characteristic can also be obtained by the same method.

Frequency responses of these additive perturbations are plotted in Fig. 5. Here, the magnitude of the uncertainty weighting function W_d is chosen to cover all the model perturbations as follows:

$$W_d = \frac{0.23(s+6)}{s+140} \cdot \frac{s+1700}{s+1000}. \tag{8}$$

Also, it is assumed that uncertainties which cannot be considered exist, and hence the magnitude of the weighting function is enlarged in the lower and higher frequency band. Since an additive perturbation is used and W_d is proper, it is noted that the assumptions of the standard H_∞ control problem is satisfied.

IV. CONTROLLER DESIGN

The design of the controller of an electrodynamic shaker is carried out using MATLAB.

A. Control objectives

Let us consider the feedback structure shown in Fig. 6. In Fig. 6, r and e_s denote the reference and the control error. The block K_b represents the controller.

The following items are set as control objectives.

- Stabilize the system even when an uncertainty exists.
- Maintain the performance wherein the reference signal is replicated well.

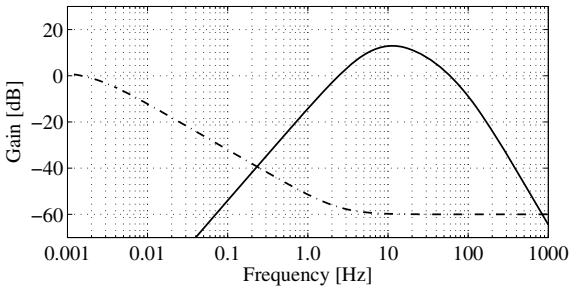

Fig. 7. Weighting function W_s and W_u. (solid line: W_s, chained line: W_u)

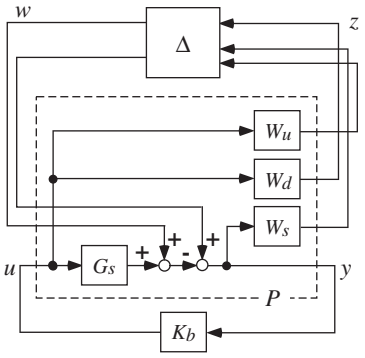

Fig. 8. Generalized plant P

A controller is designed to maintain a robust stability against the uncertainty model. Moreover, it is desired that a controller maintains a good performance despite this uncertainty. Thus, the controller for this system is designed by μ–synthesis, which has many applications like [10]. A 2DOF controller is fabricated to improve the transient response.

B. Choice of weights and μ–synthesis

A weighting function W_s for the replication performance of the reference signal is considered. It is needed that the gain of the control frequency band is enlarged to improve the control performance in the frequency band. In the acceleration control, it is noticed that the characteristic like a high pass filter is included, because this plant has zero at $s = 0$. According to the above points, W_s is now chosen as

$$W_s = \frac{10 \cdot \alpha \cdot 10 \cdot 2\pi}{s + 10 \cdot 2\pi} \cdot \frac{60 \cdot 2\pi}{s + 60 \cdot 2\pi} \cdot \frac{100 \cdot 2\pi}{s + 100 \cdot 2\pi} \cdot \frac{s}{s + 4 \cdot 2\pi} \cdot \frac{s}{s + 5 \cdot 2\pi} \cdot \frac{s}{s + 10 \cdot 2\pi}, \tag{9}$$

where, α is the adjustment parameter. α can be enlarged as long as the uncertainty is satisfied. Here, the adjustment parameter α is set at 1.0. The frequency response of the performance weighting function W_s is shown by the solid line in Fig. 7.

Practically, measuring acceleration may be influenced by noise more strongly. Hence the effect of the noise should be considered in acceleration control. Particularly, it is desired to make the magnitude of the controller low at lower frequency in this paper case. To keep the controller gain low at lower frequency, the weighting function W_u is chosen as

$$W_u = 0.001 \cdot \frac{s + 2.5 \cdot 2\pi}{s + 0.002 \cdot 2\pi}. \tag{10}$$

The frequency response of W_u is shown by the chained line in Fig. 7.

First define a block structure Δ as

$$\Delta := \left\{ \mathrm{diag}\left(\Delta_d, \Delta_{perf}\right), \Delta_d \in \mathcal{C}^{1\times 1}, \Delta_{perf} \in \mathcal{C}^{1\times 2} \right\}, \tag{11}$$

where $|\Delta_d| \leq 1$, $\|\Delta_{perf}\|_\infty \leq 1$, and Δ_{perf} is a fictitious uncertainty block for considering robust performance.

Next, it is considered that P is partitioned as

$$P = \begin{bmatrix} P_{11} & P_{12} \\ P_{21} & P_{22} \end{bmatrix}. \tag{12}$$

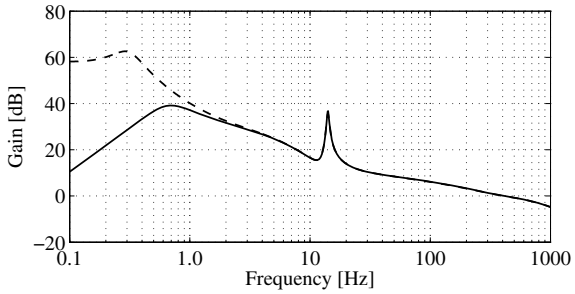

Fig. 9. Frequancy response of the controller K_b (solid line: W_u is set as (10), dashed line: $W_u = 0.0001$).

From Fig. 8, the linear fractional transportation on P by K_b is defined as follows:

$$F_l(P, K_b) := P_{11} + P_{12}K_b(I - P_{22}K_b)^{-1}P_{21}. \tag{13}$$

The robust performance condition is equivalent to the following structured singular value μ.

$$\sup_{\omega \in \mathcal{R}} \mu_\Delta \left(F_l(P, K_b)(j\omega)\right) < 1 \tag{14}$$

Since the controller satisfies this condition, the D-K iteration procedure is employed. The controller which satisfies (14) is obtained after 4 iterations, and the degree of this controller has been reduced from 29 states to 17 states. Fig. 9 shows the frequency response of the controller K_b. Also, assuming that the restriction of the control input is eased, the other controller is designed with setting W_u which is set as 0.0001, and the characteristic is shown by the dashed line in Fig. 9. Comparing to both controllers, the effect of (10) can be seen.

C. Two degrees of freedom design

To improve the system response, here a two degrees of freedom controller shown in Fig. 10 will be employed. In Fig. 10, the block F_d denotes the reference model.

In order to obtain the precise replication in the frequency band in which an accurate control performance is desired, an appropriate characteristic is selected as F_d. It is noticed that $G_s^{-1}F_d$ should be proper. Furthermore, since the magnitude of $G_s^{-1}F_d$ is not enlarged too much, it is also desired that the magnitude of the reference model F_d is small at lower

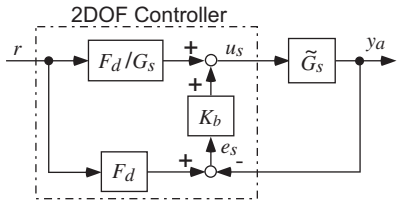

Fig. 10. Two degrees of freedom structure.

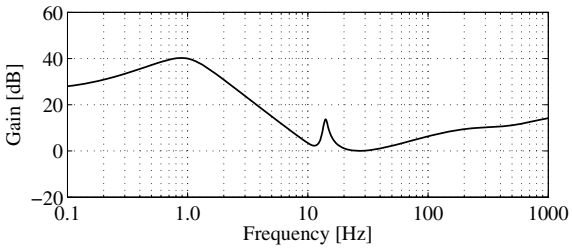

Fig. 11. Frequancy response of $G_s^{-1}F_d$.

frequency in the acceleration feedback. Then using both high-pass and low-pass filters, F_d is chosen as

$$F_d = \frac{s^3}{s^3 + 2\cdot 2\pi + 2\left(2\pi\right)^2 + \left(2\pi\right)^3} \cdot \left(\frac{1}{s + 700\cdot 2\pi}\right)^3. \tag{15}$$

The frequency response of $G_s^{-1}F_d$ is shown in Fig. 11. The gain of $G_s^{-1}F_d$ is contained up to 40 dB.

V. EXPERIMENTAL RESULT

The control performance is confirmed by an experiment. The experiment is executed by the system described in the section 2. To implement the controller with the processing board, the controller is discretized via the Tustin transform at the sampling frequency of 5120 Hz.

A. Static performance

The frequency characteristic is measured to evaluate the control performance in the static case. In this experiment, a random waveform is inputted to the controller, and the transfer function of the closed-loop characteristic is measured by the FFT analysis. The measured transfer function is compared to the simulation result.

The results of the closed-loop characteristic are shown in Fig. 12. The 2DOF controller shown in Fig. 10 is used in this experiment. Since the nominal model differs from the actual plant, the experimental result cannot yield a similar result with the simulation at high frequency band over 90 Hz and low frequency band up to 2 Hz. However, the good result is obtained in the controlled frequency band. It appears that the design specification is satisfied in the static case.

B. Transient performance

This experiment is executed by an excitation using a measured waveform data as the reference signal. The control performance is evaluated by the result of the transient response during the excitation. The original waveform of this

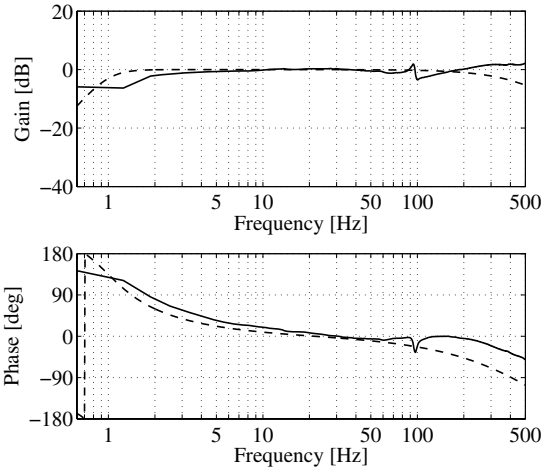

Fig. 12. Bode diagram of the closed-loop characteristic (solid line: experimental result, dashed line: simulated value)

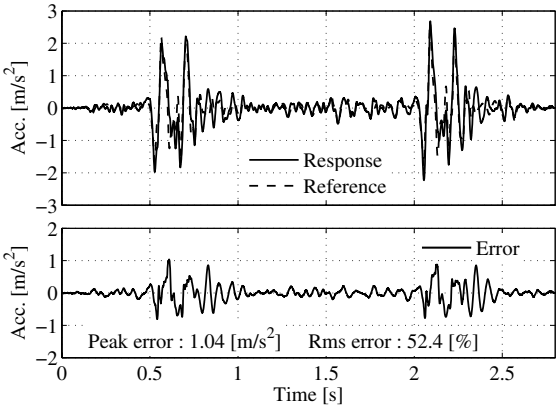

Fig. 13. Control results of the conventional controller with the first drive signal.

reference is measured at the moving vehicle. For making the reference from the original, the level of the original adjusted to be able to excitation with this shaker and the dominant frequency band are fitted to the assumed frequency band of the control.

To compare a conventional method with the proposal method, an open-loop control with the iterative excitation is also used in the experiment. The iteration process of this conventional method is summarized as follows:

1) The first drive is calculated from the measured transfer function.
2) The excitation is executed, and an error signal is obtained.
3) The next drive signal is computed from the previous drive and the error signal.
4) Go back to 2).

First, the conventional control is considered. the control results of using first drive signal are shown in Fig. 13 and those after the 4th iteration are shown in Fig. 14. The upper figure represents the reference signal which is denoted by

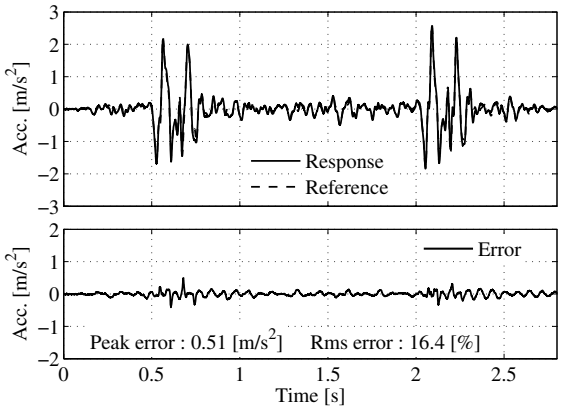

Fig. 14. Control results of the conventional controller after the 4th iteration.

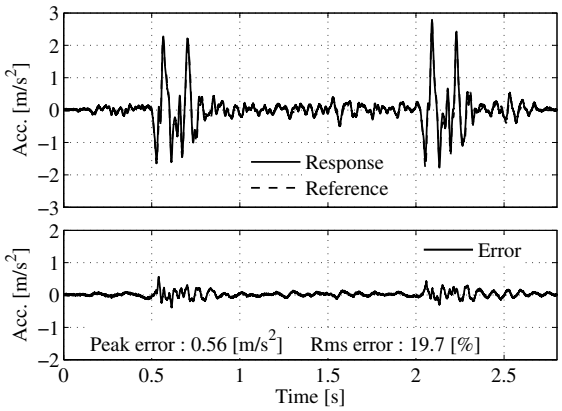

Fig. 15. Control results of the 2DOF controller.

the dashed line and the response signal which is denoted by the solid line. The lower figure shows the error signal. Because of the influence of the nonlinear perturbation of the system, it is difficult for the control using first drive signal to yield good results and the tracking error is enlarged, as shown in Fig. 13. In Fig. 14, since the drive signal is updated by the 4th iterative compensation, the waveform replication can yield a good performance as compared to Fig. 13.

Next, the proposed method is considered, the control result is shown in Fig. 15. It is shown that the response waveform yields similar results with the reference. Comparing with the results of Fig. 14, the tracking performance at the first excitation of the 2DOF controller obtains good results as well as the results after the 4th iteration of the conventional method. The power spectrum density of this control results is shown in Fig. 16. As the frequency response, the response spectrum yields similar results with the reference, and it appears that the 2DOF controller yield a good performance in the desired frequency band. Also, the rms error (= rms value of the error waveform / rms value of the reference waveform $\times$ 100 %) and the peak error are written in the control results respectively. It is found that both errors of the 2DOF controller are nearly equal to the results of Fig. 14. These results support the conclusion that this method is useful.

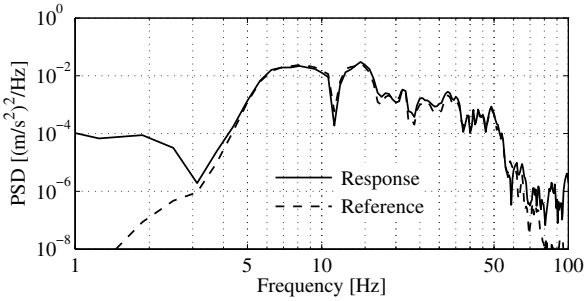

Fig. 16. Power spectrum density of the 2DOF control results.

VI. CONCLUSIONS

In this paper, the acceleration control of the electrodynamic shaker was presented. The case in which the conventional method using iterative compensation cannot be employed was considered. The proposed controller was designed by using μ–synthesis based on the remark points. Further, a two degrees of freedom controller was also designed to improve the transient response. The experiment using an actual electrodynamic shaker was shown. Then a comparison between the proposed controller and the conventional controller was shown. These results support the conclusion that the proposed acceleration controller is especially useful in the case. Although it is needed to take into account an influence of elastic modes on the shaking table in the controlled frequency band, it appears that the application of this method to a multi-axis shaking table is available.

REFERENCES

[1] K. Konagai and R. Ahsan, "Simulation of nonlinear soil-structure interaction on a shaking table," *Journal of Earthquake Engineering*, vol. 6, no. 1, pp. 31–51, 2002.

[2] A. M. Karshenas, M. W. Dunnigan, and B. W. Williams, "Adaptive inverse control algorithm for shock testing," *IEE Proceedings of Control Theory and Applications*, vol. 147, no. 3, pp. 267–276, 2000.

[3] C. M. Liaw, W. C. Yu, and T. H. Chen, "Random vibration test control of inverter-fed electrodynamic shaker," *IEEE Transactions on Industrial Electronics*, vol. 49, no. 3, pp. 587–594, 2002.

[4] D. P. Stoten and E. Gomez, "Recent application results of adaptive control on multi-axis shaking tables," in *Proc. of the 6th SECED International Conference, Seismic Design Practice into the Next Century*, 1998, pp. 381–387.

[5] A. Maekawa, C. Yasuda, and T. Yamashita, "Application of H_∞ control to a 3-D shaking table (in Japanese)," *Transactions of the SICE of Japan*, vol. 29, pp. 1094–1103, 1993.

[6] Y. Dozono, T. Horiuchi, T. Konno, and H. Katsumata, "Shaking-table control by real-time compensation of the reaction force caused by a nonlinear specimen," *Transactions of the ASME Journal of Pressure Vessel Technology*, vol. 126, no. 1, pp. 122–127, 2004.

[7] Y. Uchiyama and M. Fujita, "Application of two-degree-of-freedom control to electro-dynamic shaker using adaptive filter based on H_∞ filter," in *Proc. of the 7th European Control Conference*, Cambridge, UK, Sept. 2003.

[8] Y. Uchiyama, M. Mukai, and M. Fujita, "Robust control of multi-axis shaking system using μ-synthesis," in *Proc. of the 16th IFAC World Congress on Automatic Control*, Prague, Czech, July 2005.

[9] K. Zhou and J. C. Doyle, *Essentials of Robust Control*. Upper Saddle River, NJ: Prentice Hall, 1998.

[10] M. Fujita, T. Namerikawa, F. Matsumura, and K. Uchida, "μ-synthesis of an electromagnetic suspension system," *IEEE Transactions on Automatic Control*, vol. 40, no. 3, pp. 530–536, 1995.